

THEORY

3D Reconstruction and Volume Estimation of Jujube Using Consumer-Grade RGB-Depth Sensor

JIAN LI^{1,2}, MINGQING WU^{1,2,3}, AND HENGZHENG LI⁴¹National and Local Joint Engineering Laboratory of High Efficiency and Superior-Quality Cultivation and Fruit Deep Processing Technology of Characteristic Fruit Trees in South Xinjiang, Alar, Xinjiang 843300, China²College of Mechanical and Electrical Engineering, Tarim University, Alar, Xinjiang 843300, China³Key Laboratory of Tarim Oasis Agriculture, Ministry of Education, Alar, Xinjiang 843300, China⁴College of Mechanical and Electrical Engineering, Suzhou University, Suzhou, Anhui 234000, China

Corresponding authors: Mingqing Wu (120120006@taru.edu.cn) and Hengzheng Li (lihengzheng0216@foxmail.com)

This work was supported in part by the National and Local Joint Engineering Laboratory of High Efficiency and Superior-Quality Cultivation and Fruit Deep Processing Technology of Characteristic Fruit Trees in South of Xinjiang, China, under Grant FE201904; and in part by the Natural Science Research Project in Universities of Anhui Province, China, under Grant 2022AH051386.


ABSTRACT In order to solve the problem of three-dimensional (3D) feature measurement in grading of jujubes, a volume and surface area measurement method based on 3D point cloud registration and reconstruction was proposed. First, use the RGB-D camera to collect the multi angle point cloud data of jujubes and perform filtering processing on it. Then, the Random Sample Consensus (RANSAC) algorithm was used to fit the plane and cylinder. After fitting, divide and remove the plane point cloud, obtain the central axis parameters of the cylinder, rotate the jujube around the central axis of the cylinder at a fixed angle, and collect the images of jujube from the same perspective, The Fast Point Feature Histogram (FPFH) and Sample Consensus Initial Alignment (SAC-IA) algorithms were used to complete the 1/4 point cloud registration, the point to surface Iterative Closest Point (ICP) algorithm is used to complete the entire 1/2 registration, and the reconstructed jujube point cloud model is intercepted by the pass through algorithm. Finally, the jujubes point cloud model was smoothed and was filled of holes. The 3D coordinate method and convex hull method were used to calculate the jujube volume surface area. The correlation coefficients of the volume were 74.4 % and 74.5 %, and the correlation coefficients of the surface area was 83.2 % and 77.7 %. The experimental results show that this method can effectively calculate the 3D characteristic parameters of jujube, and can provide a reference for phenotype measurement and classification of jujube.

INDEX TERMS Cloud registration, 3D reconstruction, jujube, RGB-D camera, volume and surface area.

I. INTRODUCTION

Due to its unique geographical environment and climatic conditions, jujube produced in Xinjiang, China are the high-quality, but the grading technology is outdated and doesn't meet the current development of the economy development [1], [2]. Currently, there are three method grading artificial, mechanical and machine vision grading methods for jujube grading. Among them, The mechanical method, Which mainly relies on the long-diameter grading, has the disadvantages of a single method and low accuracy [3]. With the development of machine vision technology, there has been

a lot of research on fruit grading using RGB images [4], [5]. However, RGB images only reflect the two dimensional (2D) characteristics of fruit long diameter and projection area. Due to the difference of eigenvalues from different perspectives, RGB Image cannot reflect the real size and depth information of fruit, which will reduce the grading accuracy of fruit. Therefore, many of scholars have introduced the 3D information of fruit into the research of fruit recognition and grading. In order to realize the real-time recognition, positioning and grading of navel orange fruit by picking robot, Liu et al. [6] used RGB-D camera to realize the real-time recognition, positioning and grading of navel orange fruit. Chen et al. [7] used a Kinect camera to capture point cloud data of apples from multiple angles for fast, accurate

The associate editor coordinating the review of this manuscript and approving it for publication was Mingbo Zhao .

and non-destructive measurement of apple shape parameters, and proposed a Point cloud segmentation (PointSeg) method and migration learning algorithm-based estimation of apple phenotype parameters.

The volume and surface area are important 3D physical characteristics of agricultural products. The volumes is usually measured by Archimedes drainage method, and the surface area is obtained by peeling and slicing. This method is time-consuming, laborious and inaccurate. At present, most of the jujube sold on the market is whole jujube. The appearance of jujube with large fruit and full grains is the first choice for consumers to buy. The volume of jujube is the key point for consumers to pay attention to and an important indicator to consider whether to buy or not. The jujube processing enterprises grade jujube according to the volume of jujube, the value and price of different grading jujube were obvious [8]. In recent years, many literatures have studied the measurement methods of volume and surface area of irregular agricultural products. Sa'ad et al. [9] approximated mangoes as cylinders and used the cylinder parameters as the independent variable to build a model to predict the mass with an average error of less than 5 %. Jana et al. [10] divided fruits and vegetables into two parts along the central axis, extracted edge contour points, fitted the edge contour points using polynomials and calculated the volume by integrating the polynomials, and the experimental results showed that the accuracy of volume estimation was 92.54 %, 88.82 % and 92.84 % for potato, citrus and tomato respectively.

To obtain a complete model of the object under test, a complete coordinate system has to be set up, a complete cloud of data points formed, and visualization operations performed. When reconstructing agricultural products in 3D, placing the object on the rotating disk for rotation is necessary different viewpoints or the same viewpoints to shoot the object [11]. Wu et al [12].used rotating discs to obtain 2D images of dates at different angles, extracted the 2D on tour of jujube, reconstructed the 3D contour model of jujube with 2D outline, and calculated the volume and surface area of jujube with the outline model.

In order to quickly and non-destructively measure the 3D morphology of the maize cob, Wang et al. [13] used a powered rotary discs to collect the point cloud of the maize cob at multiple angles, and an RGB-D camera to collect the point cloud data image of the maize cob, and used the ICP alignment method to align the complete cob point cloud data, and the aligned point cloud was merged to create a 3D point cloud of the maize cob to calculate the volume of the cob using the scattering principle.

Chen et al. [14] proposed a scanning scheme that uses multi-angle line lasers scanning scheme for the evaluation of shape required in the online grading process of apples. The three-group scanning and measuring module images acquisition device with a circular distribution of six angles acquires apple 3D point cloud data and performs stitching and fusion

merges to achieve accurate measurement and classification of apple shape geometric parameters and morphology. The above algorithm has been reported to have challenges with suffers from a complex and low accuracy.

Center calibration was required before registration in order to obtaining the relative position of the coordinate of the turntable center prior to testing. Obtain accurate registration of the center axis. point clouds Nowadays, there are many methods to calibrate the central coordinate axis between the turntable and the camera, but most of them need to place additional reference objects on the turntable, Calibration objects such as calibration ball [15], cylinder [16], calibration plate [17], etc.

Currently, many scholars have proposed to use the electric rotating disk to obtain the multi-angle point cloud image of the object, calculate the central axis of the electric disk, and the point cloud was registered around the central axis, which can improve the registration accuracy and efficiency. The primary purpose of point cloud registration is to calculate the R (rotation matrix) and T (translation vector) coordinate transformation parameters according to the dislocation between the two points clouds, so as to minimize the distance of the 3D jujube measured from the two angles of view after the coordinate change [18]. The jujube has a smaller shape and less curvature variation on the surface compared to other fruits. Obtaining the reference the central axis of the reference increases the accuracy of the alignment, and because the rotation angle was known, the alignment results were more accurate and efficient compared to other alignment methods [19], [20], [21]. Zhu et al. [22] used the RANSAC algorithm to fit the cylindrical flowerpot, so as to obtain the rotation center axis parameters based on the center axis parameters, the initial registration of multi-angle. The points clouds can be completed. The point-to-surface ICP algorithm was be used to complete the fine registration, and the 3D point cloud image of the complete potted money tree is obtained.

The 3D point cloud technology is widely used in the 3D reconstruction and grading of agricultural fruit classes, but there are problems such as expensive equipment and large computational effort. This project uses a consumer-grade 3D sensor type camera, and takes jujube from the Aksu region of Xinjiang, China as the research object. this paper, a new research method is proposed, which mainly takes Aksu Jun jujube as the research object. The RGB-D camera is used to detect the center axis coordinates of the cylinder, and the point cloud is rotated according to the center axis. The initial matching, fine matching, straight-through filtering, smoothing, holes filling, filtering and reconstruction are used to obtain a complete point cloud image of jujube. Finally, the coordinate method and convex hull method are used to detect the volume and surface area of jujube, so as to solve the problem of insufficient information and lack of depth information in the grading process of jujube.

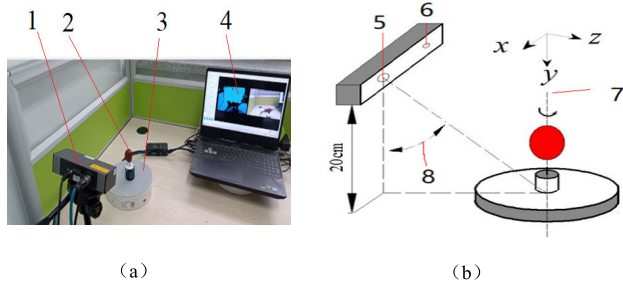


FIGURE 1. Schematic diagram of image acquisition angle (a) Physical diagram (b) schematic diagram 1. MV-3DC-120 depth camera 2. Jujube 3. Rotating disc 4. Computer 5. RGB sensor 6. Depth sensor 7. Angle 8. Rotation 9. Angle.

II. MATERIALS AND METHODS

A. INSTRUMENTS AND EQUIPMENT AND INFORMATION ACQUISITION

The RGB-D array consumer-grade scanning camera of the MV-3DC series of China's Weishi Vision Co. was selected. The projection mode of the camera is full field ultrafast laser coding, which can directly output 2-15 HZ 3D point cloud, clouds in the form of ply. The working distance of the camera is 750 mm, the optimal working distance is 500 ± 250 mm, and the square angle is $H 52^\circ \times V 31^\circ$, accuracy ± 0.5 mm@ 500 mm, supports alignment of the depth map and RGB map. Use the 3D Viewer visualization tool provided by Weishi Vision Co., to directly collect point clouds.

The Visual Studio 2019 (VS2019) development environment and point cloud library 1.12 version (PCL) were integrated to complete relevant algorithms and test simulation. The samples Jun jujube was collected and purchased from the round farms around for the experiment is from Alar, Xinjiang, China, for experiment on one-grade indicators. and according to local enterprise standards, the number of the sample were 30, with a length and diameter range of 32 mm-36 mm [23] To assess the volume of the jujube, an overflow cup and measuring cylinder were used. First, the surface of the jujube were wrap with tin foil, then the surplus part were cut off, finally unfold the tin foil, the sum of the pixels of the tin foil image were measured, and the surface area of the jujube was calculated according to the calibration method.

The 3D point cloud platform showed in Figure 1, is mainly composed of a computer, a Weishi MV-3DC 120 (MV120) cameras, and a motor rotating disc. The rotating disc has a diameter of 20 cm and rotates at an angle of 45° . Each rotation is paused for 3 seconds. A cylinder wood block with a diameter and height of 4 cm is located at the center of the disc, and a steel needle with a height of 3 cm is fixed at the center of the cylinder support the bottom of the jujube. The MV120 camera is locked on a tripod face the center of rotation, The camera lens plane is adjusted to a certain angle with the rotating disc, and the angle is calculated using an algorithm. Horizontal height from the rotating disc is 20 cm. The point cloud image is manually acquired at this angle.

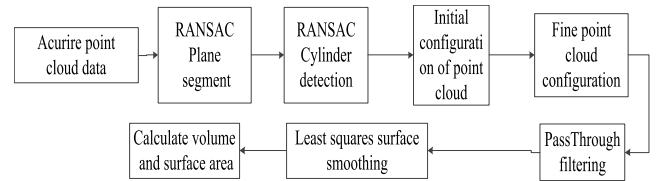


FIGURE 2. Flow chart of 3D reconstruction of jujube.

A 3D modeling method of jujube based on automatic point cloud registration is proposed, which can simulate the rolling process of jujube online grading, and achieve high-precision, low-cost non-destructive measurement.

The RANSAC algorithm is used to removes the horizontal disc surface and detects the central axis of the cylinder for the acquisition of multi-frame point cloud images a single viewpoints, the data is superimposed and merged to reduce the on the sensor to noise impact, and point cloud reconstruction is completes of the point cloud through the initial alignment and fine alignment Figure 2 shows the alignment and reconstruction the jujube image. The point cloud image of the cylinder on the rotating cone was first acquired starting from a single view, and then the RANSAC algorithm was used to segmented the image and using the RANSAC algorithm to remove the point cloud of the rotating disc under the small cylinder and detect the central axis of the small cylinder. Second, point cloud images above the jujube was rotating from a single angle, and the jujube points cloud were superimposed and fused to reduce the influence of noise on sensor noise, Point cloud reconstruction was completed through initial alignment and fine alignment. Finally, the volume and surface area of the model are calculated.

B. PREPROCESSING OF POINT CLOUD DATA

The point cloud data acquired by RGB-D camera are susceptible information beyond its intended focus length such as tables, walls and other objects, which can negative affect the subsequent point cloud model segmentation and registration. Therefore, it is necessary to remove redundant background and noise. One method of removing background noise is to delimit the spatial range of interest and sets the point cloud outside the spatial range as invalid point cloud and remove it in the process. The limiting condition set the z-axis range of 3D space within 200 mm -300 mm according to the space size of the collection platform and the sample. This paper mentioned a method that can be able to remove effectively redundant background regions from the region of interest.

The noise in this experiment mainly includes blank points, outliers, redundant background, others, different filtering methods should be applied for different noise. The blank point occur due to the instrument itself, which determine the total number of points for acquisition. If the instrument fails to acquire any points, the coordinate of X-Y-Z is displayed as zero. The zero point cloud is removed by the remove NaN method provided by PCL for acquisition (NaN is a

class of values of numerical data types in computer science, representing undefined values.). Outlier points are filtered by the radius contour line outlier removal filter [24]. There are discrete points around the collected point cloud, also called outliers, in addition, StatisticalOutlierRemoval filtering (SORF) method [25], which uses statistical methods to remove outliers. The maximum radius of the set retrieval is 5 mm, and the number of points is less than 10 will be judged as cluster points.

In this experiment, 10 pairs of point cloud images were acquired at each angle. The point cloud images were overlapped and fused from different views within at 360°. However, the density of the overlapped and fused point cloud is too large, which affects the processing speed, the ApproximateVoxelGridvoxel (AVG) filtering method was used, which approximates several points within each small cube by its center. This method obtains the point cloud needs to be used for down sampling. This method obtains the point cloud according to the center point of each voxel and does not depend on whether there is a point cloud in each voxel, resulting in higher accuracy than voxel grid [26], [27].

C. POINT CLOUD REGISTRATION

The point cloud images of the surface of the circular table and the cylinder were collected with the camera, as shown in Figure 3 a, from these image we can be observe that the cylinder axis normal vector direction spatial distribution, Y axis and Z axis. We can be seen that the detection plane of the cylinder has a certain tilt angle around the X axis, This tilt angle can be determined by calculating the angle between the X-axis and X' was 42.8°, which is the X direction vector value in the cylinder axis, and the X direction vector value can be converted into the rotation angle of the point cloud, X axis and X' As shown in Figure 3 b. The angle between the X axis and X' was 42.8° as shown in Figure 3 b. To calculate this angle, we first obtained the unit normal vector of the cylinder (0.9959, 0.8613, -0.624), the radius of 21.31 mm and any point on the central axis (93.18, 36.64, 320.51) were first obtained by fitting the cylinder. next, we used an arctangent function was used to convert the X-direction normal vector into a rotation angle, i.e., shown in Equation 1.

$$44.84^\circ = \frac{(\text{atan}(0.9959) \times 180)}{\pi} \quad (1)$$

In the above formula (1), atan represent the inverse trigonometric function.

Finally, the detected angle is used to rotate the point cloud on the surface of the cylinder and the disk, and the results are shown in Figure 3(c), which shows that the axis of the center coordinates of the cylinder is aligned with the upper horizontal surface of the cylinder, and the Z-axis ± X-axis ± Y-axis. Using the single angle cylindrical point cloud collected by the point cloud camera, the method of Cylindrical Fitting (CF) of point cloud data was used to detect the characteristic parameters such as the normal vector of the cylinder, the radius and any point of the central axis, and the

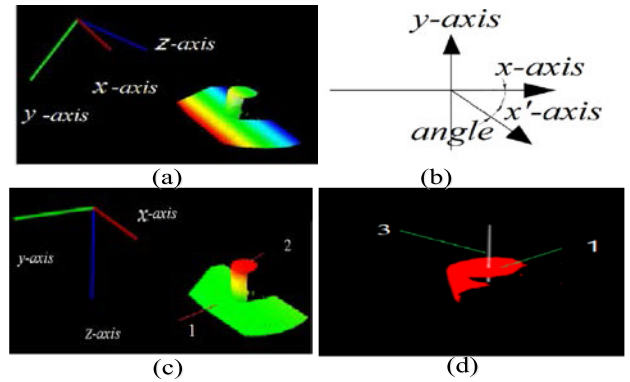


FIGURE 3. Schematic diagram of cylinder normal detection(a) x-y-z coordinate in the initial state of the camera(b) The angle of rotation of the x-axis in the coordinate system (c) Effect of the x-y-z coordinate system on the horizontal plane of the cylinder(d) Generate rendering of the central axis of a cylinder. 1. Plane, 2. Cylinder, 3. Center axis.

tilt correction of the cylindrical point cloud was realized by using the normal vector of the X-axis. After repeated experiments and accumulating certain experience, when moving the cylinder on the rotating disc, in order to obtain the unit normal vector of the center axis of the cylinder, it is necessary to use manual mode to adjust the camera coordinate system and convert the detected X-axis unit normal vector to an angle close to 45° and positive value. Meanwhile, changing the background color of the rotating disc from white to black can increase the accuracy and speed of detecting the center axis line of the cylindrical table. Knowing the point on the line and the direction vector of the line, a standard straight line for algorithm testing can be generated according to mathematical principles. The linear parameter equation is shown in Equation 2.

$$\begin{cases} x = x_0 + kt \\ y = y_0 + mt \\ z = z_0 + nt \end{cases} \quad (2)$$

where x_0, y_0 and z_0 are any point passing through on the line; k, m and n are the straight line direction or line's slope;

Take a point on the straight line as the center point to generate a spatial straight line point cloud with 5000 points, where spacing between adjacent points is 0.1 m., Set k, m equals 0, n equals -0.624. The method Compute3DCentroid (C3DC) was used for Compute the centroid of the cylinder of point cloud, which was then subtract the cylinder point cloud from the centroid coordinates, and then offset. The cylinder center axis was generated by taking the direction vector of the previous point of the cylinder axis and the axis generates the cylinder center axis, as showed in Figure 3(d).

After the above processing, rotate the point cloud around the central axis of the cylinder at a fixed angle, and observe the registration of the point cloud according to the central axis of the cylinder, as showed in Figure 4. The angle interval of the rotating disc has several fixed settings: 1/2 (180°), 1/4 (90°), 1/8 (45°) and 1/16 (22.5°). Because 180° and 90° are

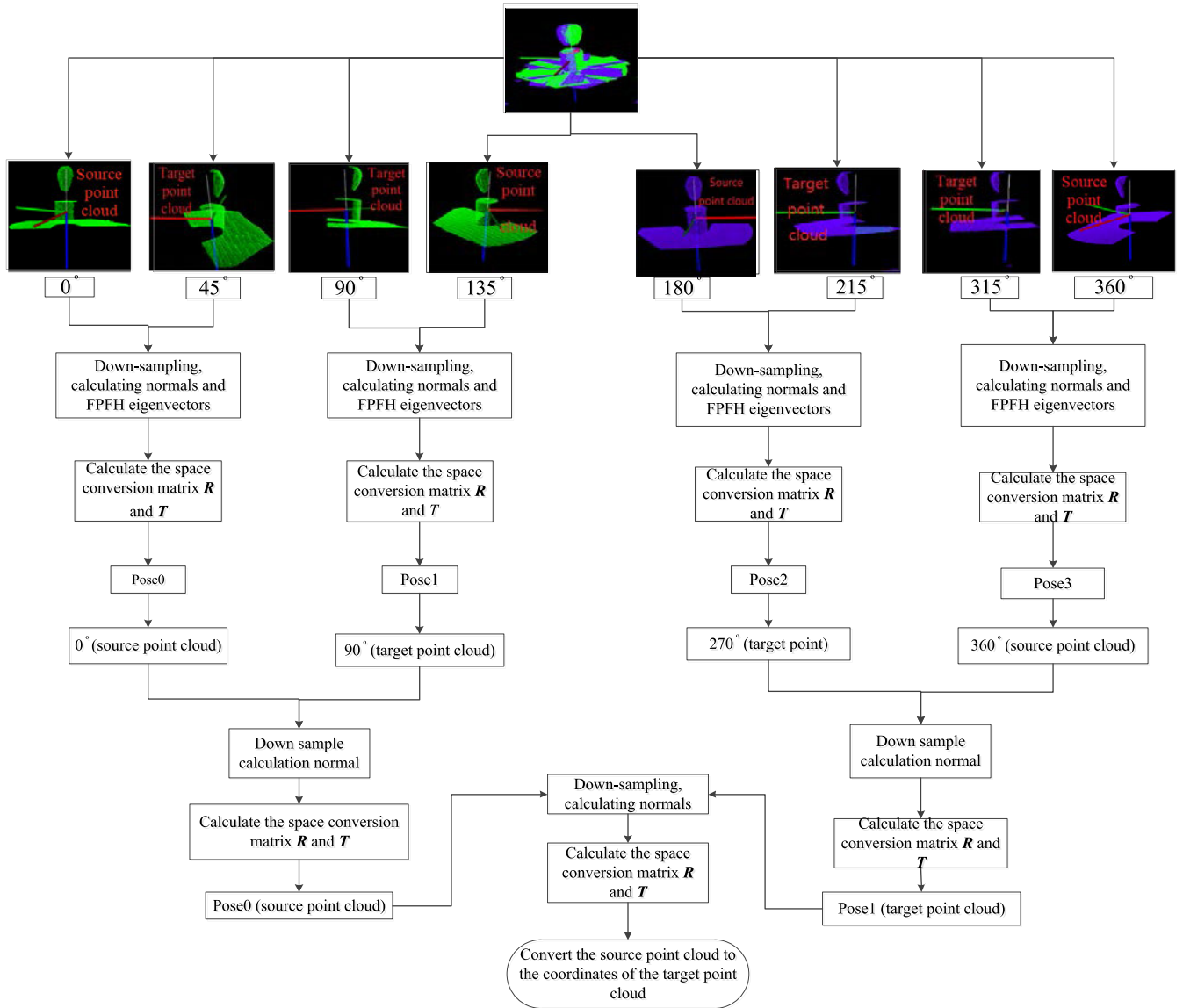


FIGURE 4. Flow chart of point cloud registration.

too small and 22.5° is too large, the final choice is an $1/8$ angle.

First, down-sampling the jujube point cloud collected by the camera from 8 angles, then extracting the surface features of two point clouds using the Fast Point Feature Histograms (FPFH) feature detection method, The feature are then used the SAC-IA algorithm to obtain the spatial transformation relationship R and T from the source point cloud to the target point cloud, thereby completing the rough registration of the point cloud, secondly, the ICP algorithm was used to complete the precise registration. With 45° and 90° point clouds as the target point clouds, the 0° and 135° source point clouds are respectively aligned with 45° and 90° target point clouds respectively, with the 210° and 315° point clouds as the target, the 180° and 360° point clouds were respectively aligned with 210° and 315° achieving $1/8$ point cloud registration. The target point clouds are rotated 45°

and -45° respectively. The point-to-plane ICP algorithm is used again, aiming at 90° and 270° point clouds, aligning 0° point cloud to 90° point cloud, and aligning 360° point cloud to 270° point cloud to achieve $1/4$ point cloud registration; Finally, the FPFH algorithm and SAC-IA algorithm were used to achieve the initial registration, and the point-to-plane ICP algorithm was used to achieve the fine registration. Combined with the 0° point cloud as the target, the 360° source point cloud is rotated 180° and aligned to the 0° point cloud, and the $1/2$ point cloud registration is completed, which is the final registration.

D. POINT CLOUD REGISTRATION ALGORITHM

1) FPFH FAST POINT FEATURE HISTOGRAM

When dealing with 3D point clouds captured from different angles of view, it is necessary to essential identify invariant features that can be used for matching between point clouds.

Point Feature Histogram (PFH) [28] is a method that uses his a histogram of the angle between the normal vectors of neighborhood points in order to describe the geometric properties of the query points. As shown in Formula 2 and Figure 5, in order to calculate the difference between two points, a coordinate system is defined based on these two given points, u - v - w is defined based on the given two points and, and the normal lines and; Define a coordinate system with u - v - w is then estbablishd, with unit vectors are u , v , and w , and following the rules specified in formula (3):

$$\begin{cases} u = n_1 \\ v = u \times \frac{p_2 - p_1}{\|p_2 - p_1\|} \\ w = u \times v \end{cases} \quad (3)$$

where $\|p_2 - p_1\|$ are the Euclidean distance between two points; w , u , v , is the unit vector

$$\begin{cases} \alpha = v \cdot n_2 \\ \phi = \frac{u \cdot p_2 - p_1}{\|p_2 - p_1\|} \\ \theta = \arctan(w \cdot n_1, u \cdot n_2) \end{cases} \quad (4)$$

where α , Φ and θ is between n_1 and n_2 of angle, The rules were set up as follows by calculateing (α , Φ , θ) parameter for all points in the k neighborhood, all parameters in the original information can be covered. Two points. (α , Φ , θ) also known as triple, triple (α , Φ , θ), then placed into its corresponding range in the histogram to form the final PFH feature expression, as shown in Formula 4. Each eigenvalue in three tuples (α , Φ , θ) is divided into b equal parts, resulting in a b^3 dimensional histogram, where each dimension correspondsto a specific range ofvalue, The frequency of the eigenvalues in each sub-interval was then counted.The typical value to b is equal to 5, which the characteristic value is divided into 5 equal parts, so the PFH feature is a vector of 125. FPFH is a simplified form of PFH [26]. Where the feature vector is is reduced from 125 to 33. Unlike PFH, FPFH does not consider the relationship between neighborhood points, but instead only takes into account the angle between the normal of query points and neighborhood pointss.

2) INITIAL REGISTRATION OF POINT CLOUD

In this paper, we use SAC-IA and the consistent initial registration algorithm [29], which adopted the registration strategy of “coarse first and then fine”. The FPFH features was used to find the matching point pairs, find an approximate transformation matrix, and execute the initial registration of the point cloud, the specific operation is as follows.

a: SAMPLING

Select n sampling points from the source point cloud P , the sampling points have unique from FPFH, and the distance between the two sampling points is greater than the preset minimum distance threshold d .

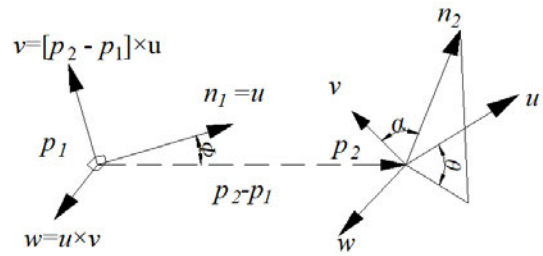


FIGURE 5. Normal vector angle of neighborhood points.

b: SELECT MATCHING POINTS

We search form multiple points in the target point cloud Q with similar FPFH features as the sampled points in the source point cloud P , and randomly select several pairs of matching point.

c: CALCULATE THE RIGID BODY TRANSFORMATION MATRIX BETWEEN POINT PAIRS

Huber function was obtained by solving the “sum of distance errors” of the i group of points, which serves to evaluated performance of registration transformation. Huber error is denoted as $H(e_i)$, as showed in Formula 5.

$$H(e_i) = \begin{cases} \frac{1}{2} \|e_i\|^2 & \|e_i\| \leq t_e \\ \frac{1}{2} t_e (2 \|e_i\| - t_e) & \|e_i\| > t_e \end{cases} \quad (5)$$

where e_i is the distance error of the i group of point clouds. t_e is the threshold value of distance error.

On this basis, we repeat the above three steps to select the transformation matrix with the smallest Huber error, Levenberg-Marquardt algorithm was used for local optimization to complete the transformation of the initial matrix.

3) POINT CLOUD ALGORITHM IS BASED ON ICP

Following FPFH rough matching and SAC-IA fine registration, We subsequently applied the iterative closest point (ICP) algorithm [30], The ICP algorithm distinguished for its simplicity and high accuracy [31].and it operates by identifying the nearest point in the target point cloud Q to the source point cloud P with Euclidean distance serving as a constraint condition The basic principle of is to find the nearest point of the current point as the constraint condition. Using these matching points, iterative algorithm the optimal transformation matrix R and T that the error function E is minimized. The error function is showed in formula (6-7).

$$E(R, T) = \frac{1}{n} \sum_{i=1}^n \|q_i - (Rp_i + T)\| \quad (6)$$

where n are number of neighborhood point cloud points, p_i is a point in the source point cloud, q_i is a point in the target point cloud, R and T are the optimal transformation matrix. The ICP algorithm has strict requirements for the initial position of the point cloud which can lead to local optima easy. Many scholars have proposed an improved algorithm. The traditional ICP algorithm uses the Euclidean distance

between two points as the error function [32].

$$E(R, T) = \frac{1}{n} \sum_{i=1}^n ||q_i - (Rp_i + T)N_i||^2 \quad (7)$$

where N_i are the normal vector of source points cloud.

For smooth surface objects, that is, point-to-point ICP algorithm can reduce matching error and accelerate convergence speed.

E. MEASUREMENT OF VOLUME AND SURFACE AREA BY COORDINATING METHOD AND CONVEX HULL METHOD

Regular objects can be calculated using conventional volume formula can be used to calculate volume of Regular objects, however in the fruit grading process, for example, apples [33], mangoes [34], pears [35], and other measured objects are often irregular, requiring bespoke formulas for volume calculation In this paper, in order to calculate the volume of irregular objects, the greedy projection triangulation algorithm was used to triangulate the surface of the filtered point cloud model, which can well reconstruct the complex topological structure we also adopt a surface reconstruction algorithm.to obtain n triangles, with the coordinate value by calculating according to the triangle the coordinates of each triangle [36], [37].We determined the volume and surface area of irregular object. According to the determinant principle and vector principle, calculate the volume of any polyhedron using the 3D space coordinates value. Specifically in the 3D space, the vertex coordinates of any triangle $\Delta A_1A_2A_3$ as $A_1(x_1, y_1, z_1), A_2(x_2, y_2, z_2), A_3(x_3, y_3, z_3)$, which were inserted into the determinant showed in formula (8).

$$\begin{vmatrix} x_1 & x_2 & x_3 \\ y_1 & y_2 & y_3 \\ z_1 & z_2 & z_3 \end{vmatrix} \quad (8)$$

where $\Delta A_1A_2A_3$ is called determinant, which is abbreviated as $d(A_1A_2A_3)$, that is,

$$d(A_1A_2A_3) = \begin{vmatrix} x_1 & x_2 & x_3 \\ y_1 & y_2 & y_3 \\ z_1 & z_2 & z_3 \end{vmatrix}$$

For $\Delta A_1A_2A_3$, there are 8 determinants in total Abbreviation $d(A_1A_2A_3)$, there is $d(A_1A_2A_3), d(A_3A_1A_2), d(A_2A_3A_1), d(A_1A_3A_2), d(A_2A_1A_3), d(A_3A_2A_1)$. Apparently, $d(A_1A_2A_3) = d(A_2A_3A_1) = d(A_3A_1A_2) = -d(A_1A_3A_2) = -d(A_2A_1A_3) = -d(A_3A_2A_1)$.

According to vector theory $d(A_1A_2A_3)$ is equal to the mixed product of $\vec{OA}_1, \vec{OA}_2, \vec{OA}_3$ and $|d(A_1A_2A_3)| = 6V(OA_1A_2A_3)$

The volume of a 3D space polyhedron is equal to 1/6 of the positive determinant of the polygons on all its faces, that is, for a 3D space polyhedron $A_0A_1A_2 \dots A_m$, the volume shown in formula (9).

$$V_{\text{volume}} = (A_0A_1 \dots A_k \dots A_m) = \frac{1}{6} \sum d(A_0A_1 \dots A_k \dots A_m) \quad (9)$$

where V_{volume} is the polyhedral volume

$A_0A_1 \dots A_k \dots A_m$ are space polyhedron single volume.

According to Helen’s formula [38] the shape surface area of a single triangle in the model can be calculated, as shown in formula (10)

$$S_{\Delta} = \sqrt{p(p-a)(p-b)(p-c)} \quad (10)$$

where S_{Δ} is the surface area of a single triangle ; a, b, c are the three sides of the triangle; p is half the circumference

$$S_{\Delta\text{surface}} = S_i + S_{i+1} + S_{i+2} \dots i = 0, 1 \dots n \quad (11)$$

where $S_{\Delta\text{surface}}$ is surface area of spatial polyhedron;

$S_i + S_{i+1} + S_{i+2}$ is surface area of a single triangle;

To utilize PCL, We first declare a PCL ConvexHull `<pcl::Point<XYZ>` type method, and input the filtered point cloud data into the method, We then use the reconstruct function to reconstruct the 3D point cloud model, to obtain the volume and surface area of the point cloud model We employ the the `getTotalArea` and `getTotalVolume` functions. to obtain the volume and surface area of the point cloud model,by applying convex hull algorithm [39]. We can calculate the volume and surface area of the model The specific declaration method is as follows.

```
pcl::ConvexHull<pcl::PointXYZ> Convex_hull_Volume
andSurface;// Declare a method for calculating convex hull
pcl::ConvexHull<pcl::PointX-Y-Z> Convex_hull_Volume
andSurface;// Declare a method for calculating convex hull
std::vector<pcl::Vertices> hull_polygon;// Declare a
vector
Convex_hull_VolumeandSurface.setInputCloud(cloud_
hull);
Convex_hull_VolumeandSurface.reconstruct(*cloud_hull,
hull_polygon1);
double volume_hull = Convex_hull_VolumeandSurface.
getTotalVolume();// Calculate the volume of 3D
double area_hull = Convex_hull_VolumeandSurface.get
TotalArea();// Calculate the surface area of 3D
```

F. EVALUATION INDEX OF REGISTRATION EFFECT

To evaluate the automatic registration performance, this paper proposes two kinds of assessment metrics valuation indicators, overlap rate and root mean square error of distance.

1) OVERLAP RATE

The successful registration of two point clouds is achieved by they overlap, complementing each other and share common points. The number of duplicate point clouds in two parts affects the quality of point clouds of the registration. Generally, the greater the overlap rate of point clouds, the better the matching effect. The calculation method of overlapping rate was shown in formula (12):

$$R_{\text{overlap}} = \frac{P_{\text{src}}}{P_{\text{tgt}}} \times 100\% \quad (12)$$

where R_{overlap} represents the proportion between the source point cloud and the target point cloud after registration, which

is the overlap rate, p_{src} are matching points in source point cloud and target P_{tgt} are total number of source points cloud and target point cloud

2) ROOT MEAN SQUARE ERROR OF DISTANCE

Calculating accuracy the distance error between corresponding points in two point clouds after registration, it is necessary to verify the accuracy of registration. Other words, better registration results are indicated by smaller the distance namely the REMS. formula (13) defines the REMS.

$$RMSE = \sqrt{\frac{\sum_{i=1}^n (x_i - \hat{x}_i)^2}{n}} \quad (13)$$

In the above formula(13), n is denotes the number of corresponding points; x_i is represent Euclidean distance between corresponding points after registration; \hat{x}_i is the true value of the Euclidean distance between the corresponding points. Assuming complete registration, the valid value is 0.

III. EXPERIMENTAL RESULTS AND ANALYSIS

A. POINT CLOUD REGISTRATION PROCESSES

Figure 6a showed the point cloud registration process for jujube To start, we rotate the point cloud 45° to complete the initial transformation, as depicted in Figure 6a position, with the white line was the central axis of the cylinder. We then employed the coarse The point clouds were registered using the coarse FPFH, Fine SAC-IA and ICP algorithms for point cloud registration, and registration and fusion of two point clouds (1/8) are presented in Figure 6b, next, we rotated target by 45° in the reverse direction, applied point-to-point ICP algorithm, and obtained the registered and fusion of two (1/8) were present in Figure 6c. The two point clouds (1/4), the red point cloud is the source point cloud, and the green point cloud is the target point cloud were separated by angle of 90°. We registered point cloud using coarse FPFH and fine SAC-IA and point-to-point ICP algorithm and the result of registered fusion of two point clouds (1/4) is illustrated in Figure 6d, with an include angle 180° between the two points; Point-to-point ICP algorithm was be used, the results of two point (1/2) registration and fusion, and results are displayed in Figure 6e, with an included between angle two point clouds of 180°.

The jujube model point cloud image of was segmented by the pass-through algorithm of the straight-through filter. After matching, there were holes at the bottom of the jujube point-cloud. In this study we utilized Geomagic12 version software to fill the holes, and then the point cloud model data of the segmented jujube was smoothed and hole-repaired using a point cloud resampling method based on moving least squares. After filling, registration, resampling, smoothing, and hole repair, the contour of the jujube was more complete. We then applied Greedy Projection Triangle (GPT) algorithm for projection, as exemplified in in Figure 6 f, we selects a sample triangle as the initial surface, continuously expands the surface boundary, ultimately forming a

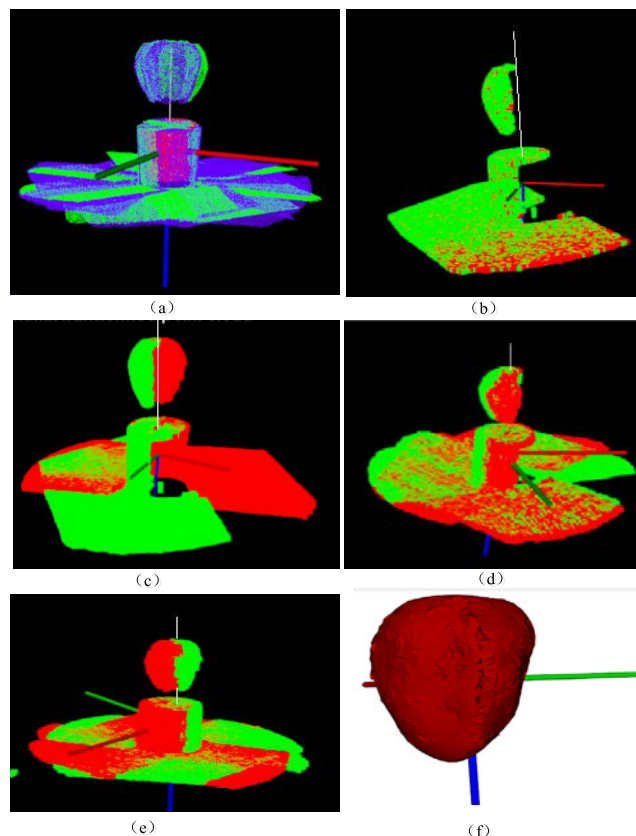


FIGURE 6. 3D registration and reconstruction registration process of jujube (a) Initial point cloud (b) 45° FPFH & SAC-IA registration (c) 90° point to surface ICP registration (d) 180° FPFH & SAC-IA registration (e) Point to surface 180° ICP registration (f) Greedy projection triangulation algorithm.

complete triangular surface mesh, and finally, we extract the coordinates of the triangular mesh to calculate the volume and surface area.

B. ANALYSIS OF POINT CLOUDS REGISTRATION ACCURACY

The point cloud registration process requires manual setting of adjustment parameters, and reasonable parameter settings can enhance the registration effect. We conducted registration tests using The purpose is carrying registration tests, which take 1 from 15 jujube point clouds, and the point cloud Pose0 as an example. The results were presented in Table 1. The distance error after initial registration was 2.46 cm-3.56 cm, and the average time consumed after rough registration was 9.68 s; The distance point cloud after fine registration was 1.8-1.05 cm, the average time consumed is 0.013, and the REMS was 0.72 cm; After rough registration, the preset precision was achieved. showing the importance of rough registration for fine registration.

Setting an appropriate down sample voxel size was crucial to improve the registration accuracy. experiments show that the larger the voxel size resulted in in fewer point cloud after down sampling, and the shorter the registration time. We set

TABLE 1. Registration time and accuracy comparison.

Point cloud group number	Number of points of source point cloud and target point cloud	Automatic registration total time/s	Rough registration Time/s	Accurate registration time/s	Root mean square error/cm
1	2442/2791	19.30	19.27	0.028	0.77
2	2814/2610	7.45	7.43	0.024	0.67
3	2758/2497	7.68	7.65	0.024	0.76
4	992/956	3.96	3.95	0.010	0.76
5	2396/2384	13.54	13.52	0.018	0.83
6	1054/1043	17.14	17.13	0.006	0.79
7	1054/1043	4.93	4.92	0.004	0.76
8	964/923	4.26	4.25	0.011	0.75
9	981/1008	4.39	4.39	0.006	0.76
10	963/956	4.30	4.29	0.004	0.72
11	851/860	30.20	30.19	0.006	0.73
12	2618/2446	11.89	11.86	0.035	0.78
13	2726/2642	11.69	11.67	0.015	0.68
14	969/907	4.73	4.72	0.005	0.78
15	1012/1004	5.78	5.77	0.006	0.72

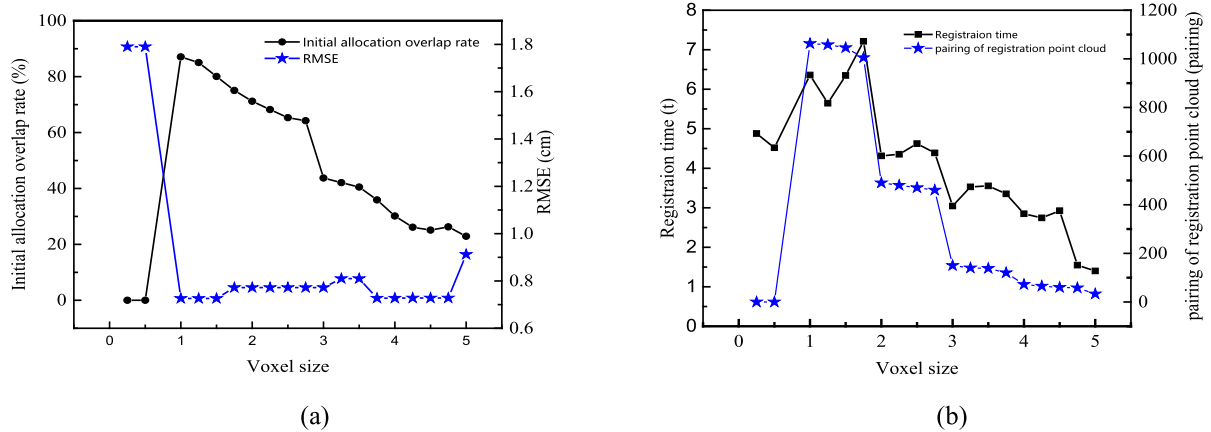


FIGURE 7. Effect of voxel size on initial registration results (a) Trend Chart of Point Cloud Voxel Size Change with Initial Matching Overlay (%) and RMSE (cm) (b) Trend chart of point cloud Voxel size change with registration time (t) and Logarithm (Pair) of registration points.

the voxel size range between 0-5 and the registration overlap rate and root meansquare error is calculated. The voxel size was incremented in steps of 0.25. Figure 7a display the relationship between the voxel size in the range of 0.25-5. and the registration overlap rate and RMSE Figure 7b illustrate relationship between voxel size in within the range of 0-5, rough matching time, and number of matching pairing.

Alignment results indicate that the RMSE decreases with the increase of voxel size and tends to level off after reaching a certain value, while the overlap rate of alignment is smaller with the increase of voxel size; the time consumed time of alignment is inversely. proportional to the number of corresponding points and voxel size as showed in Figure 8(a-c). proportional to the number of corresponding points and voxel size. Considering the accuracy and efficiency of the alignment, the point set stability and differentiation are better when the voxel size is taken as 2.

C. MEASUREMENT AND ANALYSIS OF VOLUME AND SURFACE AREA

In this paper utilized drainage method and image method to assess the surface area of jujube. The drainage method

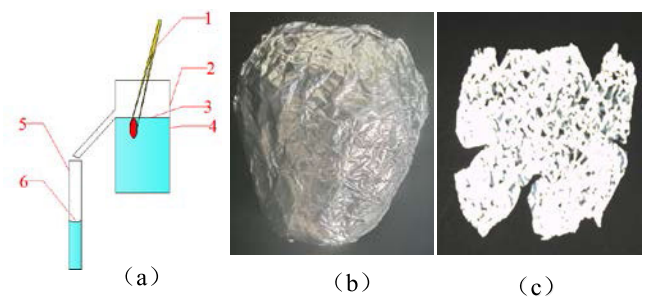


FIGURE 8. Schematic diagram of jujube volume and surface area measurement (a) Measurement of jujube volume by drainage method (b) measurement of jujube surface volume by tin paper surface sticking method (c) after the tin foil is unfolded 1. Tweezers 2. Beaker 3. Residual water level 4. Jujube to be tested 5. Discharge water level 6. Measuring cylinder.

involved clamping the jujube into the overflow cup using tweezers, with the measuring cylinder receiving the overflow water and corresponding scale. There are 6 mm×6 mm squares on A4 paper. was used to calibrate the pixel distance and establish the proportional relationship between the pixel value and the real value. Subsequently the jujube surface was

TABLE 2. Measurement results of three methods for jujube, (Note, 1 milliliter (ml) = 1 cubic centimeter (cm³)).

Num	Measuring area by image method/cm ²	Volume measurement by drainage method/ml	Surface measurement by convex hull method/cm ²	Measuring volume by convex hull method/cm ³	Measuring surface area by coordinate method/cm ²	Measuring volume by coordinate method/cm ³
1	48.35	21.50	44.69	26.66	46.41	25.79
2	56.77	24.00	46.90	27.62	52.01	26.28
3	44.94	19.50	45.57	27.13	46.65	25.10
4	57.82	30.00	66.15	45.61	68.37	42.50
5	44.76	23.00	48.87	39.39	63.10	36.87
6	50.40	24.00	49.65	30.32	58.13	28.10
7	77.07	25.00	73.01	55.56	76.42	52.30
8	40.67	16.00	36.39	19.16	44.48	17.34
9	52.19	21.00	57.37	38.37	64.43	36.91
10	45.68	20.00	43.73	25.31	45.91	22.86
11	57.64	19.00	47.73	27.29	55.44	21.91
12	42.41	18.00	45.76	26.85	45.94	24.81
13	51.43	21.00	50.78	32.11	53.31	30.78
14	49.76	24.00	53.89	34.12	56.64	30.91
15	56.91	26.50	60.49	41.01	64.44	38.87

wrapped with tin foil minimized. The bwarea function from Matlab software R2020a version was used to count the number of pixels then cut, unfold and flatten it on the white paper, and minimize the cut surface tin foil and calculate the surface area. n, so as to Fifteen jujubes were assessed using both the drainage method and image method and measurement results are presented in Table 2.

IV. CONCLUSION

Three methods were used to measure the volume of jujube, the correlation coefficient between drainage method and convex hull method was 74.4 %, and that between drainage method and coordinate method was 74.5 %; For measure the surface area, the correlation between image method and convex hull method was 83.2 %, and the correlation between image method and coordinate method being 77.7 %. Both the convex hull method and the coordinate method were utilized to calculate the volume and surface area of jujube. The precision of calculating the volume was similar between two methods, but the convex hull method has higher precision than the coordinate method.

Compared with traditional drainage method and image method, the convex hull method and coordinate method were found more convenient, rapid and non-destructive for measuring the volume and surface area of jujube. Additionally, these methods have promising application prospects in 3D feature parameter measurement and grading. In this study jujube was selected as the research object, with MV120 cameras and electric rotary disc utilized for constructing the acquisition platform. The relevant algorithms were completed using the PCL integrated development environment based on VS2019. The central axis of the cylinder was identified by random sampling consistency algorithm, followed by point cloud image registration and reconstruction.

1) This paper proposes an approach for the rough and fine registration of jujube point cloud images by pfph, sacia and point-to-point icp algorithms. An evaluation index system is also proposed to verify the accuracy and efficiency

of registration, which enables automatic registration of point clouds. The mean time of rough registration is 9.68 s, while the mean time of fine registration is 0.013 s, with a mean root mean square error of 0.72 cm. The rmse initially increases and then decreases with the increase of voxel size, and then tends to be flat after reaching a certain value. The overlap rate of registration decreases with the increase of voxel size; registration time is inversely proportional to the corresponding number of points and a reasonable voxel size of 2 for down sampling (2 is voxel size) was set to effectively reduce error accumulation caused by iteration in the registration process.

2) This paper the convex hull and coordinate method for measuring the volume and surface area of jujube, producing comparable results. The correlation of the two methods for volume measurement were 74.4% and 74.5 %, and the surface area correlation are 83.2 % and 77.7 %, respectively. These results meet the requirements and can be applied to the volume measurement of jujube agricultural products. The algorithm in this paper provides a technical reference for the research of 3d reconstruction, 3d features parameter measurement and classification based on jujube in xinjiang region of china.

REFERENCES

- [1] Z. Guo, H. Zheng, X. Xu, J. Ju, Z. Zheng, C. You, and Y. Gu, "Quality grading of jujubes using composite convolutional neural networks in combination with RGB color space segmentation and deep convolutional generative adversarial networks," *J. Food Process Eng.*, vol. 44, no. 2, Dec. 2020, Art. no. e13620.
- [2] C. Hai, F. Zhao, and S. Sun, "Research on online detection for jujube surface defects based on blob analysis," *Food. Mach.*, vol. 34, no. 1, pp. 126–129, Jan. 2018.
- [3] F. Y. Bai, G. X. He, G. J. He, H. G. Liu, and L. S. Wang, "Research progresses of red jujube automatic grading machines," *Ningxia Eng. Technol.*, vol. 15, no. 1, pp. 88–92, Mar. 2016.
- [4] H. Wang, "Grading method of jujube based on image edge detection," *J. Agric. mech. Res.*, vol. 40, no. 1, pp. 231–234, Oct. 2018.
- [5] B. Z. Yan and L. Xiong, "Research on quality classification of jujube based on computer vision technology," *J. Agricult. Mech. Res.*, vol. 40, no. 8, pp. 232–235, Aug. 2018.
- [6] E. D. Liu, L. Zhu, Z. W. Ji, and L. Yue, "Real-time identification, localization, and grading method for navel oranges based on RGB-D camera," *Trans. Chin. Soc. Agric. Eng.*, vol. 38, no. 14, pp. 154–165, Jul. 2020.

- [7] L. Chen, Y. H. Wang, M. C. Ji, and L. H. Xu, "Estimation algorithm of apple phenotypic parameters based on pointnet and transfer learning," *J. Nanjing Agric. Univ.*, vol. 44, no. 6, pp. 1209–1216, 2021.
- [8] Z. Lou, Q. Liu, F. J. Shi, Q. Yu Zhao, and Q. Z. Gao, "Air impingement drying shrinkage characteristics of Chinese jujube," *Trans. Chin. Soc. Agric. Mach.*, vol. 45, no. S1, pp. 241–246, Nov. 2014.
- [9] F. S. A. Sa'ad, M. F. Ibrahim, A. Y. M. Shakaff, A. Zakaria, and M. Z. Abdullah, "Shape and weight grading of mangoes using visible imaging," *Comput. Electron. Agricult.*, vol. 115, pp. 51–56, Jul. 2015.
- [10] S. Jana, R. Parekh, and B. Sarkar, "A De novo approach for automatic volume and mass estimation of fruits and vegetables," *Optik*, vol. 200, Jan. 2020, Art. no. 163443.
- [11] H. L. Zheng, H. L. Wang, J. M. Wang, and H. R. Yi, "Automated. 3D reconstruction of leaf lettuce based on Kinect camera," *Trans. Chin. Soc. Agric. Mach.*, vol. 52, no. 7, pp. 159–168, Jul. 2021.
- [12] Q. M. Wu, K. X. Yi, P. H. Luo, F. C. Li, Y. X. Tang, and J. K. Chen, "On-line measurement method for, volume and surface area of red jujube based on multi-contour model," *Trans. Chin. Soc. Agric. Eng.*, vol. 35, no. 19, pp. 190–283, Oct. 2019.
- [13] K. Wang, Z. Ge, H. Guo, R. H. Zhang, L. Chen, and H. T. Quan, "3D shape indexes measurement system of maize ear based on Xtion sensor," *Transducer. Microsyst. Technol.*, vol. 34, no. 4, pp. 62–65, Jan. 2015.
- [14] G. Q. Chen, Q. Liu, C. J. Zhang, and H. K. Wu, "Easurement and classification of apple shape based on multi-view three-dimensional vision imaging," *J. Hangzhou. Dianzi. Univ. Nat. Sci.*, vol. 42, no. 4, pp. 34–41, Jul. 2022.
- [15] H. Liu, K. C. Pan, Y. Shen, and B. Gao, "Plant point cloud information fusion method based on SICK and Kinect sensors," *Trans. Chin. Soc. Agric. Mach.*, vol. 49, no. 10, pp. 284–291, Oct. 2018.
- [16] A. Y. Xu, Q. Yang, and P. J. Huai, "Calibration of the axis of the turntable in 4-axis laser measuring system and registration of multi-View," *Chin. J. Lasers*, vol. 32, no. 5, pp. 659–662, May 2005.
- [17] Z. Langming, Z. Xiaohu, and G. Banglei, "A flexible method for multi-view point clouds alignment of small-size object," *Measurement*, vol. 58, pp. 115–129, Dec. 2014.
- [18] P. Ou and D. Wang, "A desktop three-dimensional scanning technology based on line structured light," *Opt. Instrum.*, vol. 39, no. 4, pp. 25–33, Aug. 2017.
- [19] X. Wang, Q. X. Zhang, and K. Y. Guo, "Experimental analysis of multi angle point cloud stitching algorithm," *Digital. Technol.*, vol. 40, no. 7, pp. 12–14, Jul. 2022.
- [20] Z. Z. Han, Y. X. Wang, Y. Y. Liu, and Z. Matthias, "Ulti-angle point cloud-VAE: Unsupervised feature learning for 3D point clouds from multiple angles by joint self-reconstruction and half-to-half prediction," in *Proc. IEEE/CVF Int. Conf. Comput. Vis. (ICCV)*, Oct. 2019, pp. 10441–10450.
- [21] B. Li, Z. Li, and F. X. Wang, "A rapid registration method based on multi-angle point cloud data," *Digital. Techno. Appl.*, vol. 40, no. 4, pp. 12–14, Feb. 2022.
- [22] B. Q. Zhu, M. Zhang, F. Z. Liu, and C. X. Li, "Identification and counting method of potted kumquat fruits based on point cloud registration," *Trans. Chin. Soc. Agric. Mach.*, vol. 53, no. 5, pp. 216–290, May 2022.
- [23] Q. M. Wu, F. C. Li, P. H. Luo, K. X. Yi, and S. A. Shakeel, "Physical characteristics of red jujube in different grades and its influence on classification results," *Trans. Chin. Soc. Agricult. Machinery*, vol. 49, no. 8, pp. 324–330, Aug. 2018.
- [24] G. Li, T. Fu, and C. T. Zhang, "Research on point cloud registration method of mine environment based on PCL," *J. Mach. Des.*, vol. 38, no. S1, pp. 174–177, Jan. Jul. 2021.
- [25] H. Chen, H. Zhang, C. Liu, Y. Chai, and X. Li, "An outlier detection-based method for artifact removal of few-channel EEGs," *J. Neural Eng.*, vol. 19, no. 5, Oct. 2022, Art. no. 056028.
- [26] B. Zhou, H. Min, and Y. Kang, "Research on 3D point cloud segmentation algorithm in PCL environment," *Microelectron. Comput.*, vol. 35, no. 6, pp. 101–105, Jun. 2018.
- [27] M. Andries, A. Dehban, and J. Santos-Victor, "Automatic generation of object shapes with desired affordances using voxelgrid representation," *Frontiers Neurobot.*, vol. 14, p. 22, Apr. 2020.
- [28] R. B. Rusu, N. Blodow, Z. C. Marton, and M. Beetz, "Aligning point cloud views using persistent feature histograms," in *Proc. IEEE/RSJ Int. Conf. Intell. Robots Syst.*, Sep. 2008, pp. 22–26.
- [29] Y. Lin, Q. Li, and T. Chen, "Point cloud registration of tree based on FPFH," *J. Chin. Agric. Mech.*, vol. 43, no. 2, pp. 155–162, Feb. 2022.
- [30] P. J. Besl and N. D. McKay, "A method for registration of 3-D shapes," *IEEE Trans. Pattern Anal. Mach. Intell.*, vol. 14, no. 2, pp. 239–256, Feb. 1992.
- [31] Y. D. Ren, J. X. Li, T. Lin, M. M. Xiong, H. Z. Xu, and J. G. Cui, "3D reconstruction method for fruit tree branches based on Kinect v2 sensor," *Trans. Chin. Soc. Agric. Mach.*, vol. 53, no. S2, pp. 197–203, Aug. 2022.
- [32] L. K. Low, "Linear least-squares optimization for point-to-plane ICP surface registration," Chapel Hill Univ. North Carolina, Feb. 2004, pp. 1–3, vol. 4.
- [33] S. Yamamoto, M. Karkee, Y. Kobayashi, N. Nakayama, S. Tsubota, L. N. T. Thanh, and T. Konya, "3D reconstruction of apple fruits using consumer-grade RGB-depth sensor," *Eng. Agricult., Environ. Food*, vol. 11, no. 4, pp. 159–168, Oct. 2018.
- [34] T. Mon and N. ZARAug, "Vision based volume estimation method for automatic mango grading system," *Biosyst. Eng.*, vol. 198, pp. 338–349, Oct. 2020.
- [35] A. G. Moreno, M. Forero, F. Gomez, and R. Mauricio, "Hass avocado classification by color and volume using a Kinect sensor," in *Proc. SPIE*, Aug. 2019, pp. 465–471.
- [36] X. M. Liu and Y. J. Cui, "Calculate, volume of complex objects based on 3D coordinates of point cloud data," *J. Geomatics.*, vol. 43, no. 3, pp. 96–98, Jun. 2018.
- [37] J. Wei, "A coordinate computing method of the three-dimensional space arbitrary polyhedron, volume," *J. Hu zhou. Teach. Coll. Nat. Sci.*, no. 5, pp. 67–73, Jun. 1996.
- [38] P. F. Ou and C. L. Li, "Eetrahedron, volume formula similar to Helen's formula," *Res. Math. Teach.*, vol. 1, no. 4, pp. 25–27, 1984.
- [39] C. B. Barber, D. P. Dobkin, and H. Huhdanpaa, "The quickhull algorithm for convex hulls," *ACM Trans. Math. Softw.*, vol. 22, no. 4, pp. 469–483, Dec. 1996.



JIAN LI received the bachelor's degree in theoretical and applied mechanics and the master's degree in solid mechanics from the Lanzhou University of China, in 2009 and 2012, respectively. He is currently pursuing the Ph.D. degree in solid mechanics with Wuhan University, China. Since 2015, he has been a Teacher with the School of Mechanical and Electrical Engineering, Tarim University, China. His research interests include agricultural machinery engineering mechanics and data-driven computational mechanics.



MINGQING WU received the S.M. degree in agricultural machinery mechanization engineering from Gansu Agricultural University, in 2009, and the Ph.D. degree in agricultural machinery mechanization engineering from Nanjing Agricultural University, in 2020. He is currently an Associate Professor with Tarim University, China. His primary research interests include artificial intelligence and 3D point clouds.



HENGZHENG LI received the Ph.D. degree in agricultural mechanization engineering from Nanjing Agricultural University, China, in 2019. He is currently an Associate Professor with Suzhou University, China. His primary research interests include agricultural equipment and automatic control.

...